# PROCEEDINGS OF SPIE

SPIEDigitalLibrary.org/conference-proceedings-of-spie

# Hyperspectral imaging microscopy for measurement of localized second messenger signals in single cells

Thomas C. Rich, J. R. Griswold, Joshua Deal, Naga Annamdevula, Kathleen McAlister, et al.

Thomas C. Rich, J. R. Griswold, Joshua Deal, Naga Annamdevula, Kathleen McAlister, Samuel Mayes, Craig Browning, Marina Parker, Silas J. Leavesley, "Hyperspectral imaging microscopy for measurement of localized second messenger signals in single cells," Proc. SPIE 10881, Imaging, Manipulation, and Analysis of Biomolecules, Cells, and Tissues XVII, 108811F (4 March 2019); doi: 10.1117/12.2508052



Event: SPIE BiOS, 2019, San Francisco, California, United States

# Hyperspectral imaging microscopy for measurement of localized second messenger signals in single cells

Thomas C. Rich<sup>1,2</sup>, JR Griswold<sup>4</sup>, Joshua Deal<sup>1,2</sup>, Naga Annamdevula<sup>1,2</sup>, Kathleen McAlister<sup>3</sup>, Samuel Mayes<sup>4</sup>, Craig Browning<sup>4</sup>, Marina Parker<sup>4</sup>, and Silas J. Leavelsey<sup>1,2,4</sup>

<sup>1</sup>Pharmacology, University of South Alabama, AL 36688

<sup>2</sup>Center for Lung Biology, University of South Alabama, AL 36688

<sup>3</sup>Biomedical Sciences, University of South Alabama, AL, 36688

<sup>4</sup>Chemical and Biomolecular Engineering, University of South Alabama, AL 36688

## **ABSTRACT**

Ca<sup>2+</sup> and cAMP are ubiquitous second messengers known to differentially regulate a variety of cellular functions over a wide range of timescales. Studies from a variety of groups support the hypothesis that these signals can be localized to discrete locations within cells, and that this subcellular localization is a critical component of signaling specificity. However, to date, it has been difficult to track second messenger signals at multiple locations within a single cell. This difficulty is largely due to the inability to measure multiplexed florescence signals in real time. To overcome this limitation, we have utilized both emission scan- and excitation scan-based hyperspectral imaging approaches to track second messenger signals as well as labeled cellular structures and/or proteins in the same cell. We have previously reported that hyperspectral imaging techniques improve the signal-to-noise ratios of both fluorescence and FRET measurements, and are thus well suited for the measurement of localized second messenger signals. Using these approaches, we have measured near plasma membrane and near nuclear membrane cAMP signals, as well as distributed signals within the cytosol, in several cell types including airway smooth muscle, pulmonary endothelial, and HEK-293 cells. We have also measured cAMP and Ca<sup>2+</sup> signals near autofluorescent structures that appear to be golgi. Our data demonstrate that hyperspectral imaging approaches provide unique insight into the spatial and kinetic distributions of cAMP and Ca<sup>2+</sup> signals in single cells.

**Keywords:** Hyperspectral imaging, spectral imaging, microscopy, FRET, cAMP, Ca<sup>2+</sup>, second messenger signaling, compartmentalized signals

# 1. INTRODUCTION

The development of  $Ca^{2+}$  dyes and genetically encoded cAMP and  $Ca^{2+}$  probes has allowed visualization of  $2^{nd}$  messenger signals in a variety of cell types (1-8). However, effective use of these probes has been limited by artifacts associated with the intracellular environment and, more importantly, by low signal-to-noise ratios – this is especially true for FRET-based probes, discussed in (9). In addition, low signal-to-noise ratios have effectively prohibited accurate assessment of fluorescence/FRET distributions in 3D (x,y,z) or rapid and accurate measurement of multiple probes, severely limiting the ability to interpret intracellular signaling events. Here we demonstrate that hyperspectral imaging and analysis approaches can be used to overcome such limitations.

Hyperspectral imaging approaches were developed by NASA for feature identification in satellite images. It was quickly realized that these imaging approaches offer the potential to detect multiple components in biological systems (9, 10). We previously demonstrated that hyperspectral approaches also offer improved signal-to-noise ratio for quantification of intracellular fluorophores as well as FRET signals (11-13). Here we demonstrate that hyperspectral imaging approaches allow assessment of the intracellular distribution of multiple fluorophores, allowing the measurement of signals at multiple subcellular locations within the same cell. Using this approach we were for the first time able to assess time course and magnitude of spatial cAMP gradients within pulmonary microvascular endothelial cells (PMVECs). We were also able to track cAMP signals near fluorescently labeled AKAP79, a scaffolding protein critical for signal fidelity in the cAMP signaling pathway. This study demonstrates the potential

Imaging, Manipulation, and Analysis of Biomolecules, Cells, and Tissues XVII, edited by Daniel L. Farkas, Attila Tarnok, James F. Leary, Proc. of SPIE Vol. 10881, 108811F  $\cdot$  © 2019 SPIE  $\cdot$  CCC code: 1605-7422/19/\$18  $\cdot$  doi: 10.1117/12.2508052

to use hyperspectral imaging approaches to assess second messenger signals such as cAMP at multiple discrete locations within single cells.

## 2. MATERIALS AND METHODS

#### 2.1 Cell culture

Rat pulmonary microvascular endothelial cells (PMVECs) were isolated as described previously (14) by the cell culture core of the Center for Lung Biology at University of South Alabama. PMVECs were maintained in Dulbecco's modified Eagles medium (DMEM, Life Technologies Inc.) supplemented with 10% v/v fetal bovine serum (Gemini),  $100 \mu$ g/ml streptomycin, and  $100 \mu$ ml penicillin, pH 7.0. Cells were grown in  $100 \mu$ mm culture dishes at 37 °C in a humidified atmosphere of 95% air, 5% CO<sub>2</sub>. Confluent monolayers were passaged using 1% trypsin-EDTA (Invitrogen). Experiments were performed at room temperature (20-23°C).

# 2.2 Transfection of FRET-based cAMP reporters

Human embryonic kidney (HEK-293) or pulmonary microvascular endothelial cells (PMVECs) were cultured on laminin-coated 25 mm glass cover slips. Cells were transfected with pCDNA3 plasmids encoding mCherry-labeled AKAP79 or H188 FRET-based cAMP probes using 2.5  $\mu$ g plasmid, 3.75  $\mu$ l Lipofectamine 3000, and 5 $\mu$ l P3000 (Invitrogen) per well in serum-free media. H188 is a FRET-based cAMP probe comprised of a cAMP binding domain from the EPAC protein sandwiched between a donor and acceptor (Turquoise and Venus fluorescent proteins, respectively) (5). Binding of cAMP to the probe causes a conformational change that reduces FRET efficiency. *In vitro* measurements indicate that H188 has an apparent cAMP affinity of  $\sim$  2.0  $\mu$ M. Cells were transfected with donor or acceptor alone to obtain the spectral signatures and to perform photobleaching controls. Cells were assayed  $\sim$ 48 hr post transfection.

## 2.3 Hyperspectral confocal imaging

Cells were labeled with DRAQ5 (25  $\mu$ M, 10 min) or NucBlue (1 drop/mL, 10 min) to label nuclei and washed twice with phosphate buffered saline prior to imaging. Microscopy was performed using a Nikon A1R confocal microscope. Image stacks were collected at 1  $\mu$ m intervals (z-stack) at excitation wavelengths of 405 (8% laser intensity) and 562 nm (6% intensity) and emission wavelengths ranging from 414 to 724 nm at 10 nm increments. 16 to 20 confocal slices (z slices) were acquired per image stack, depending on the height of the cell. Using these settings, total acquisition time for a confocal stack was 15 to 20 s. Following imaging of the baseline condition for 60 to 120 s, cells were exposed to 50  $\mu$ M forskolin (an adenylyl cyclase activator) or 0.1  $\mu$ M isoproterenol (a  $\beta$  adrenergic agonist), as indicated, and imaged every 30 s for 20 minutes. Single fluorophore controls were used to further assess photobleaching or other factors that could influence fluorescence emission. Little or no photobleaching was observed over the time course of these experiments. Hyperspectral image stacks were unmixed using a linear unmixing algorithm implemented in MATLAB (Mathworks). FRET levels and cAMP concentrations were calculated as described elsewhere (13, 15-17). Localized signals were estimated as described in the Results and Discussion, below. Data are representative of results from  $\geq$  4 cells.

#### 2.4 Statistics

Statistics were calculated using SigmaPlot v13. Comparisons of cAMP levels were made using a two-way ANOVA with a Tukey post hoc test;  $p \le 0.05$  was considered significant.

## 3. RESULTS AND DISCUSSION

Second messenger signals simultaneously regulate a wide variety of cellular functions. Understanding the mechanisms of signal specificity has been an area of active research for the last half century (4, 9, 18-25). However, it has been difficult to directly measure distinct second messenger signals at discrete locations in the same cell. The reasons for this are multifaceted and include a lack of spatial resolution, a lack of temporal resolution and a lack of sensitivity in second messenger measurements. In addition, the most widely used approaches for measuring localized signals involve targeting probes to discrete subcellular domains (26, 27). While this in many cases is an effective way to detect changes in second messenger signals at discrete subcellular locations, there are several limitations that must

be considered: (i) Targeting of probes effectively prohibits measuring second messenger signals near other cellular structures/proteins in the same cell. (ii) Thus, comparisons of signals in two discrete subcellular domains requires the study of signals in different cells. (iii) And, targeting creates high local concentrations of the probe that may lead to buffering of the probe, and, in the case of Förster resonance energy transfer (FRET) based probes, the potential for both intra- and inter-molecular FRET (potentially distorting the interpretation of the signal). Here, we propose a complimentary approach to study localized signals. We propose to use hyperspectral imaging approaches to measure second messenger signals adjacent to multiple cellular structures or adjacent to labeled proteins within single cells. This study further supports the use of spectral imaging technologies to study the mechanisms of signaling specificity in second messenger systems.

We sought to assess cAMP concentrations in three cellular domains in the same cell – the subplasmalemmal and perinuclear spaces and in the bulk cytosol. The H188 FRET-based probe was expressed in pulmonary microvascular endothelial cells (PMVECs) as outlined in the MATERIALS AND METHODS and described previously (13). 4D (x,y, $\lambda$ ,t) hyperspectral confocal image stacks were acquired and FRET/cAMP levels were estimated as outlined in the MATERIALS AND METHODS. Figure 1 depicts the process by which we identified the perinuclear and subplasmalemmal spaces. In brief, to identify the perinuclear space we identified the nuclear space using the DRAQ5 signal, dilated the image by 5 pixels, and then subtracted the two images to generate a mask of the perinuclear space (Figure 1A-C). Similarly, to identify the subplasmalemmal space we identified the cell periphery based upon a preset threshold for total fluorescence of the H188 probe, eroded the boundary by 5 pixels, and subtracted the two images to generate a mask of the subplasmalemmal space (Figure 1D-F). This approach allowed us to isolate FRET signals in the bulk cytosol (the entire cytosolic space), the perinuclear space, and the subplasmalemmal space (Figure 1G-I).

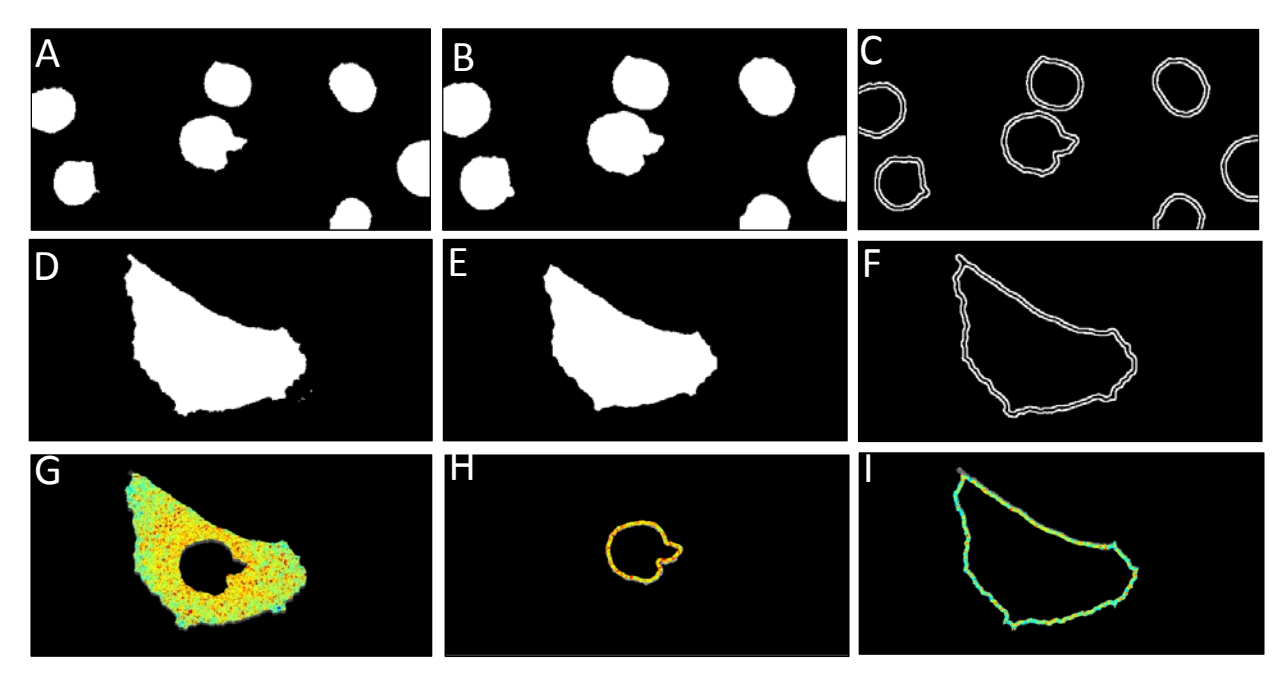


Figure 1: Segmentation of perinuclear and subplasmalemmal regions of interest. (A) A DRAQ5 binary mask image. (B) A DRAQ5 binary mask image dilated by five pixels. (C) Subtraction of (A) from (B) was used to generate the perinuclear region of interest. (D) The Turquoise + Venus mask. (E) Erosion of the the Turquoise + Venus mask by pixels. (F) Subtraction of (E) from (D) was used to generate the subplasmalemmal region of interest. (G) The cAMP signal in the entire image slice. (H)The cAMP signaling in the perinuclear region was obtained by applying the mask indicated in (C). (I) Similarly, the cAMP signal in subplasmalemmal region was obtained by applying the mask indicated in (F).

We next assessed the time course of forskolin-induced cAMP signals within each of these domains (Figures 2 and 3). A relatively stable baseline signal was observed in each of these domains. 50  $\mu$ M forskolin (an adenylyl cyclase activator) was added at 60 s. After a brief delay, forskolin induced an increase in cAMP in each of the three subcellular regions. Interestingly, forskolin triggered a transient cAMP signal in the subplasmalemmal space and in the bulk cytosol (Figure 2A,B); however, the signal in the perinuclear space continued to increase throughout the time

course of the experiment (Figure 2C). This general response was consistent across 5 PMVECs. To better quantify the response we assessed the cAMP levels at the three subcellular regions at four time points: 0, 400, 800, and 1200 seconds (Figure 3). A two-way ANOVA with Tukey post hoc indicated significant differences in cAMP levels as a function of both time and subcellular location.

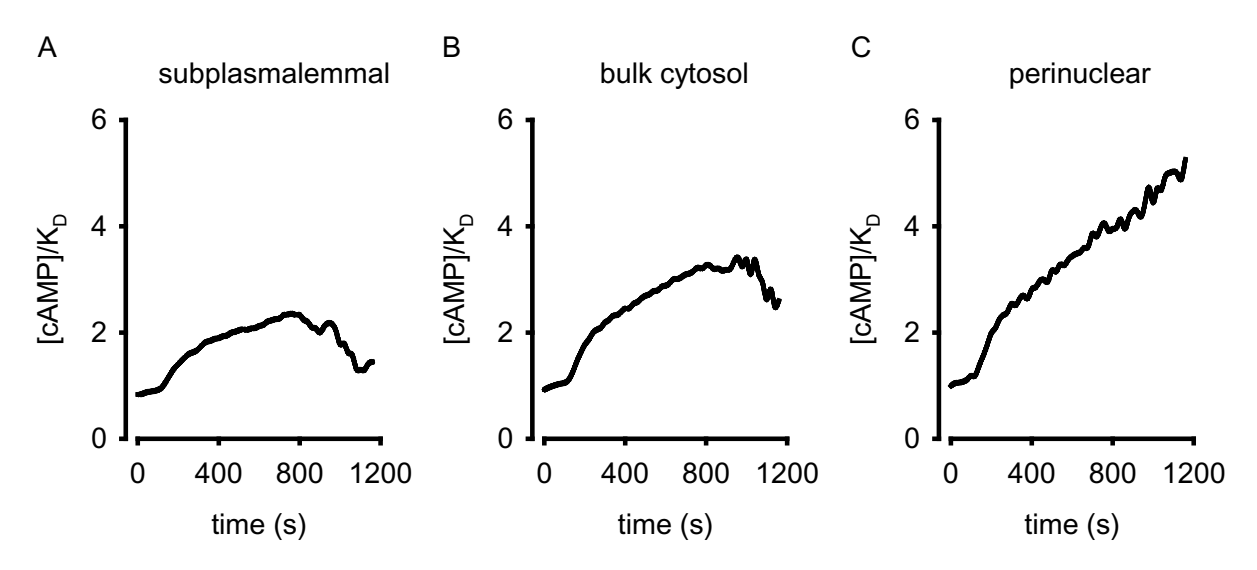


Figure 2: The time course of localized, forskolin-induced FRET signals in PMVECs. (A) The time course of cAMP signals averaged in the subplasmalemmal region of the cell, as depicted in Figure 1I. (B) The time course of cAMP signals averaged in the entire cell, described in the literature as the bulk cytosol, as depicted in Figure 1G. (C) The time course of cAMP signals averaged in the perinuclear region of the cell, as depicted in Figure 1H. These data clearly demonstrate marked differences between agonist-induced cAMP signals in distinct regions of the same cell.

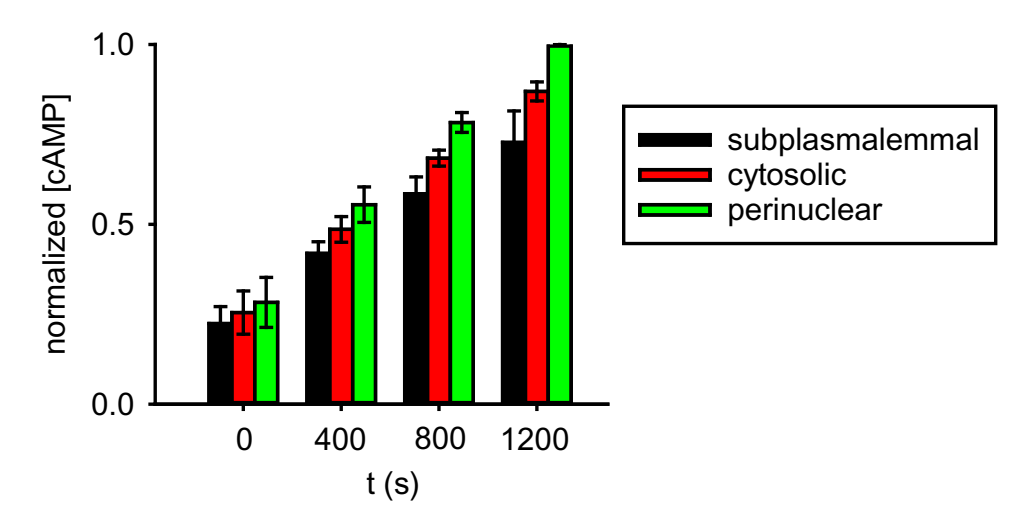


Figure 3: Normalized cAMP levels at three subcellular regions as a function of time. In order to compare cAMP levels averaged within discrete subcellular regions we assessed forskolin-induced cAMP levels in the subplasmalemmal, bulk cytosolic, and perinuclear regions of PMVECs at 4 time points: 0, 400, 800, 12000 s. A two-way ANOVA indicated significant difference in cAMP levels as a function of both time and subcellular location. These data clearly indicate that spectral imaging and image analysis approaches can be used to quantify cAMP levels at multiple subcellular locations within the same cell, n = 5 PMVECs.

Interestingly, these data indicate that forskolin triggers larger total cAMP levels in the perinuclear space than in the bulk cytosol or subplamalemmal domains of PMVECs. We interpret these results to indicate that either, forskolin is activating a pool of cAMP in the perinuclear space and/or, the apparent perinuclear origin of cAMP is due to three dimensional (3D) distributions of adenlylyl cyclase and phosphodiesterase (i.e., in x, y, and z dimensions). Indeed, our recent results suggest that forskolin-induced cAMP gradients originate from the top of PMVECs and spread downwards. Additional studies will be required to discriminate between these possibilities (13, 28).

Above, we demonstrated the ability to discern differences in cAMP levels between multiple subcellular regions. This approach allows measurement of cAMP levels near distributed structures such as the plasma and nuclear membranes. We next wanted to measure FRET levels near labeled proteins. For this experiment we chose to use HEK-293 cells due to the relative ease of transfection of multiple plasmids. We chose to measure cAMP levels near a labeled A-kinase anchoring protein (AKAP), a family of scaffolding proteins critical for fidelity in the cAMP signaling pathway. Specifically, we chose mCherry-labeled AKAP79 because AKAP79 is endogenously expressed in HEK-293 cells. Expression patterns of labeled AKAP79 are shown in red in Figure 4A, nuclei are labeled in blue. AKAP79 appears to have a largely near-membrane distribution, consistent with previous reports (29-32). Figure 4B shows the distribution of baseline FRET efficiency near labeled AKAP79, indicated by hot colors (red and orange). Addition of the β adrenergic agonist isoproterenol (0.1 μM at 60 s) triggered a marked decrease in FRET efficiency, indicated by cooler colors (yellow and blue), near labeled AKAP79, consistent with an increase in cAMP levels. These experiments clearly demonstrate that we can detect changes in cAMP levels near labeled proteins in living cells.



Figure 4. FRET signals near mCherry-labeled AKAP79 in HEK-293 cells. HEK-293 cells were co-transfected with the H188 cAMP FRET probe and mCherry-labeled AKAP79. (A) The distribution of mCherry-labeled AKAP79 in HEK-293 cells. mCherry-labeled AKAP79 is depicted in red, NucBlue-labeled nuclei are depicted in blue. (B) High FRET levels, indicated by hot colors (red and orange), at the beginning of the experiment reflect low cAMP levels. (C) Low FRET levels, indicated by cooler colors (yellow and blue), reflect an increase in cAMP levels near mCHerry labeled AKAPs in response to 0.1 µM isoproterenol (added at 60 s).

# 4. FUTURE WORK

The study presented here clearly demonstrates that hyperspectral imaging and analysis approaches allow measurement of cAMP signals – and, more generally, second messenger signals – at multiple locations within a single cell. In the future, we need to address two critical issues. The first issue to overcome is the ability to make these measurement in both three spatial dimensions (3D) and in real time – or near real time. Indeed, our recent studies demonstrate a critical need to assess second messenger signals in 3D (13). The second related issue is to increase the overall signal-to-noise ratio of these measurements (33), which would in turn allow for high speed, 3D measurements of second messenger signals. We are currently investigating the use of novel excitation-scan based hyperspectral imaging technologies for this purpose (9, 34).

#### 5. ACKNOWLEDGEMENTS

We would like to thank Drs. Kees Jalink and Mark Dell'Acqua for providing constructs encoding H188 and mCherry-labeled AKAP79. The authors would also like to acknowledge support from NIH P01HL066299, R01HL137030, R01HL058506, and S10RR027535, NSF MRI1725937, and AHA 18PRE34060163. Drs. Leavesley and Rich disclose a financial interest in the start-up company SpectraCyte LLC, formed to commercialize spectral imaging technologies.

# 6. REFERENCES

- 1. G. Grynkiewicz, M. Poenie, and R. Y. Tsien, "A new generation of Ca<sup>2+</sup> indicators with greatly improved fluorescence properties," *J. Biol. Chem.* **260**(6), 3440-3450 (1985).
- 2. T. C. Rich et al., "Cyclic nucleotide-gated channels colocalize with adenylyl cyclase in regions of restricted cAMP diffusion," *J. Gen. Physiol.* **116**(147-161. PMCID: PMC2229499 (2000).
- 3. T. C. Rich et al., "A uniform extracellular stimulus triggers distinct cAMP signals in different compartments of a simple cell," *Proc. Natl. Acad. Sci. USA* **98**(13049-13054. PMCID: PMC60822 (2001).
- 4. W. Xin et al., "Estimating the magnitude of near-membrane PDE4 activity in living cells," *Am. J. Physiol. Cell Physiol.* **309** ( C415-C424. PMCID: PMC4572370 (2015).
- 5. J. Klarenbeek et al., "Fourth-generation epac-based FRET sensors for cAMP feature exceptional brightness, photostability and dynamic range: characterization of dedicated sensors for FLIM, for ratiometry and with high affinity," *PLoS One* 10), e0122513 (2015).
- 6. J. B. Klarenbeek et al., "A mTurquoise-based cAMP sensor for both FLIM and ratiometric read-out has improved dynamic range," *PLoS One* **6**(e19170 (2011).
- 7. T. A. Pologruto, R. Yasuda, and K. Svoboda, "Monitoring neural activity and [Ca2+] with genetically encoded Ca<sup>2+</sup> indicators," *J. Neurosci.* **24**(9572-9579 (2004).
- 8. E. Shigetomi, S. Kracun, and B. S. Khakh, "Monitoring astrocyte calcium microdomains with improved membrane targeted GCaMP reporters," *Neuron Glia Biol.* **6**(183-191 (2010).
- 9. T. C. Rich, K. J. Webb, and S. J. Leavesley, "Perspectives on: Cyclic nucleotide microdomains and signaling specificity: Can we decipher the information content contained within cyclic nucleotide signals?," *J. Gen Physiol.* **143**(17-27. PMCID: PMC3874573 (2014).
- 10. A. T. Harris, "Spectral mapping tools from the earth sciences applied to spectral microscopy data," *Cytometry* **69A**(872-879 (2006).
- 11. P. Favreau et al., "Tunable thin film optical filters for hyperspectral microscopy," *J. Biomed. Optics* **19**(011017. PMCID: PMC3784641 (2014).
- 12. S. J. Leavesley et al., "Hyperspectral imaging microscopy for identification and quantitative analysis of fluorescently-labeled cells in highly autofluorescent tissue," *J. Biophotonics* **5**(67-84. PMCID: PMC3517021 (2012).
- 13. N. S. Annamdevula et al., "Spectral imaging of FRET-based sensors reveals sustained cAMP gradients in three spatial dimensions," *Cytometry A* **93**(1029-1038 (2018).
- 14. T. Stevens, J. Creighton, and W. J. Thompson, "Control of cAMP in lung endothelial cell phenotypes. Implications for control of barrier function.," *Am. J. Physiol.* **277**(L119 -L126 (1999).
- 15. S. J. Leavesley et al., "Assessing FRET using spectral techniques," *Cytometry A* **83**(898-912. PCMID: PMC4374658 (2013).
- 16. T. C. Rich et al., "Hyperspectral Imaging of FRET-based cGMP probes," *Meth. Mol. Biol.* 73-88 (2013).
- 17. S. J. Leavesley et al., "Automated image analysis of FRET signals for subcellular cAMP quantification," *Methods Mol. Biol.* 1294), 59-70 (2015).
- 18. J. Jurevicius, and R. Fischmeister, "cAMP compartmentation is responsible for a local activation of cardiac Ca<sup>2+</sup> channels by b-adrenergic agonists," *Proc. Natl. Acad. Sci. USA* **93**(295-299 (1996).
- 19. L. L. Brunton, J. S. Hayes, and S. E. Mayer, "Functional compartmentation of cAMP and protein kinase in heart," *Adv. Cyclic Nucleotide Res.* **14**(391-397 (1981).
- J. D. Corbin et al., "Compartmentalization of adenosine 3':5'-monophosphate and adenosine 3':5'-monophosphate-dependent protein kinase in heart tissue," J. Biol. Chem. 252(3854-3861 (1977).
- 21. T. J. Rink, R. Y. Tsien, and A. E. Warner, "Free calcium in Xenopus embryos measured with ion-selective microelectrodes," *Nature* **283**(5748), 658-660 (1980).
- 22. R. Y. Tsien, "New calcium indicators and buffers with high selectivity against magnesium and protons: design, synthesis, and properties of prototype structures," *Biochemistry* **19**(11), 2396-2404 (1980).

- T. Pozzan et al., "Is cytosolic ionized calcium regulating neutrophil activation?," Science 221(4618), 1413-1415 (1983).
- 24. R. Y. Tsien, "Intracellular measurements of ion activities," *Annual Review of Biophysics & Bioengineering* **12**(91-116 (1983).
- D. A. Williams et al., "Calcium gradients in single smooth muscle cells revealed by the digital imaging microscope using Fura-2," *Nature* **318**(6046), 558-561 (1985).
- L. M. DiPilato, X. Cheng, and J. Zhang, "Fluorescent indicators of cAMP and Epac activation reveal differential dynamics of cAMP signaling within discrete subcellular compartments," *Proc. Natl. Acad. Sci.* USA 101(16513-16518 (2004).
- 27. L. Oldach, and J. Zhang, "Genetically encoded fluorescent biosensors for live-cell visualization of protein phosphorylation," *Chem. Biol.* **21**(186-197 (2014).
- 28. T. C. Rich et al., "Three dimensional measurement of cAMP gradients using hyperspectral confocal microscopy," *Proc. SPIE* **97130O** (doi:10.1117/1112.2213273 (2016).
- 29. R. Efendiev et al., "AKAP79 interacts with multiple adenylyl cyclase (AC) isoforms and scaffolds AC5 and -6 to alpha-amino-3-hydroxyl-5-methyl-4-isoxazole-propionate (AMPA) receptors," *J. Biol. Chem.* **285**(14450-14458 (2010)).
- 30. S. J. Tavalin, "AKAP79 selectively enhances protein kinase C regulation of GluR1 at a Ca2+-calmodulin-dependent protein kinase II/protein kinase C site," *J. Biol. Chem.* **283**(11445-11452. (2008).
- 31. M. D. Houslay, and G. S. Baillie, "beta-Arrestin-recruited phosphodiesterase-4 desensitizes the AKAP79/PKA-mediated switching of beta<sub>2</sub>-adrenoceptor signalling to activation of ERK," *Biochem. Soc. Trans.* **33**(1333-1336 (2005).
- 32. M. Cong et al., "Regulation of membrane targeting of the G protein-coupled receptor kinase 2 by protein kinase A and its anchoring protein AKAP79," *J. Biol. Chem.* **276**(15192-15199 (2001).
- 33. S. J. Leavesley, and T. C. Rich, "Overcoming limitations of FRET measurements," *Cytometry A.* **89**(325-327 (2016).
- 34. P. Favreau et al., "An excitation-scanning hyperspectral imaging microscope " *J. Biomed. Opt.* **19**(046010. doi: 046010.041117/046011. (2014).